Dipolar-Chemical Shift and Rotational Resonance ^{13}C NMR Studies of the Carboxyl−Methylene Carbon Spin Pair in Solid Phenylacetic Acid and Potassium Hydrogen Bisphenylacetate

David L. Bryce and Roderick E. Wasylishen*

Department of Chemistry, Dalhousie University, Halifax, Nova Scotia, Canada, B3H 4J3

Received: April 10, 2000; In Final Form: June 8, 2000

The dipolar-chemical shift (CS) method has been applied to analyze the carboxyl−methylene carbon isolated spin pair in phenylacetic-$^{13}C_2$ acid and potassium hydrogen bisphenylacetate-$^{13}C_2$. The span, Ω, of the CS tensor is decreased significantly for both carbon atoms in the potassium acid salt compared to the acid. The orientations of the carboxyl CS tensor and, more notably, the methylene CS tensor, have a marked dependence on the protonation state of the carboxyl group. Ab initio calculations [RHF/6-311G*, RHF/6-311++G(2d,-2p)] support the experimental findings. In addition to these studies, we demonstrate how rotational resonance (RR) NMR spectroscopy complements the dipolar-CS method in a study of the isolated ^{13}C spin pairs in phenylacetic-$^{13}C_2$ acid. In particular, the higher-order RR experiments provide a stringent check on the CS parameters and the dipolar coupling constant, *R*, derived from the dipolar-CS analysis. The dipolar-CS method, in combination with a two-dimensional spin−echo experiment, yields $R = 2150 \pm 30$ Hz for phenylacetic acid, whereas RR indicates that $R = 2100 \pm 15$ Hz. Although $n = 1$ RR can be applied reliably to determine internuclear distances in the absence of CS tensor data, these data are critical for simulations of the $n = 2$ RR effects. Specifically, longitudinal magnetization exchange curves are shown to be sensitive to slight rotations of the carboxyl carbon CS tensor about an axis perpendicular to the carboxyl plane, a phenomenon observed upon moving from the acid to the acid salt. Simulations indicate that altering the MAS rate by only a few tens of hertz can drastically alter the higher-order RR line shapes. The ab initio calculations of chemical shielding tensors provide data that are useful in the simulation of rotational resonance effects. We propose phenylacetic-$^{13}C_2$ acid as a setup sample for rotational resonance and other homonuclear dipolar recoupling experiments.

Introduction

The dipolar-chemical shift (CS) method is an effective NMR technique for studying isolated spin-$^1/_2$ pairs in stationary powdered solids.[1−6] Under favorable circumstances, when symmetry dictates the orientation of at least one component of one of the CS tensors, this method will yield the direct dipolar coupling constant (R_{DD}), the magnitudes of the principal components of the two CS tensors, the relative orientations of the CS tensors, and the orientations of these tensors with respect to the molecular axis system.[6] The fact that this orientational information is derived from a powdered sample makes the method particularly valuable when single crystals are not available. R_{DD} is of interest because of its simple relationship with the distance, r_{12}, between nucleus 1 and nucleus 2 (eq 1)

$$R_{DD} = \frac{\mu_0}{4\pi} \frac{\gamma_1\gamma_2}{<r_{12}^3>} \frac{\hbar}{2\pi} \qquad (1)$$

where μ_0 is the permeability of free space and γ_1 and γ_2 are the magnetogyric ratios of the nuclei under consideration. It is important to recognize that r_{12} is a motionally averaged distance. Complications in measuring very accurate values of r_{12} using solid-state NMR will be discussed below (vide infra). Duncan's compilation[7] lists CS principal components for many carboxyl carbons and about fifty methylene carbons, but information regarding the orientation of the methylene tensors appears to be scarce in the literature.[8] In the present work, the dipolar-CS method has been applied to the carboxyl−methylene carbon isolated spin pair in phenylacetic-$^{13}C_2$ acid and its potassium acid salt, potassium hydrogen bisphenylacetate. Specifically, one of the goals of this research is to explore the effects on the CS tensors of the protonation state of the acid. Although it is well-known that, for the carboxyl carbon, the most shielded component of the CS tensor is approximately perpendicular to the COO plane,[9a,10−13] the orientations of δ_{11} and δ_{22} in this plane will depend on subtle structural features. The effect of deprotonation of crystalline amino acids on the magnitudes of the carboxyl CS tensor principal components has been examined by Gu and McDermott;[10] however, their study made no mention of how the tensor orientation changes upon deprotonation. Furthermore, the effect of deprotonation on the CS tensor of the methylene carbon was not addressed.

The dipolar-CS method applies to stationary samples, and as discussed above, the observed spectra are strongly dependent on the CS tensors. Efforts have been focused on devising an experiment that is less dependent on knowledge of the CS tensors, yet strongly dependent on R_{DD}. Because magic-angle spinning (MAS) averages the CS tensor to its isotropic value, many techniques have been developed that allow for the reintroduction of the homonuclear dipolar interaction in an isolated spin pair under MAS conditions; these include, for

* Author to whom correspondence should be addressed. E-mail: Roderick.Wasylishen@ualberta.ca.

10.1021/jp0013661 CCC: $19.00
Published on Web 07/21/2000

example, rotational resonance,[14−17] DRAMA,[18] SEDRA,[19] RFDR,[20] USEME,[21] CROWN,[22] 2Q-HORROR,[23] MELODRAMA,[24] R2TR,[25] C7,[26] DRAWS,[27] R^2T,[28] APPR,[29] and the newly introduced SPC-5.[30] Rotational resonance (RR) is a particularly appealing technique because of the simplicity of the experimental conditions. No special pulse sequences are required; rather, the MAS rate must be adjusted such that, when it is multiplied by an integer, the product is equal to the difference in isotropic chemical shifts between the two spin-$^1/_2$ nuclei of interest. This condition is summarized in the RR equation[14,15]

$$n\nu_{rot} = (\nu_1^{iso} - \nu_2^{iso}) \quad n = 1, 2, 3, ... \tag{2}$$

When the RR condition is satisfied, the homonuclear dipolar interaction is reintroduced, and a pronounced broadening or splitting of the usual MAS peaks is observed.[14−16] Additionally, a rapid oscillatory exchange of Zeeman magnetization occurs between the two spins. Usually, it is the profile of this exchange as a function of time that is simulated to extract R_{DD}. A technique for reintroducing the quadrupolar interaction under MAS conditions has been proposed recently.[31]

Although the RR phenomenon was first recognized many years ago by Andrew et al.,[14] its recent renaissance[17,32−46] can be attributed to its rediscovery in 1988 by Raleigh et al.[15] Experimentally, the drawbacks of the RR technique include the fact that very stable sample spinning is required and that the range of suitable differences in isotropic chemical shifts is limited by eq 2. Newer developments such as R2TR,[25] rotational resonance tickling (R^2T),[28] and multiple-pulse scaled RR[47] have overcome some of these difficulties. The reintroduction of the direct dipolar interaction between a pair of homonuclear half-integer quadrupolar spins has been described recently.[48,49] Hodgkinson and Emsley have addressed the issue of multiple-spin interactions and their effect on the accuracy of homonuclear and heteronuclear distance measurements in solid-state NMR.[50]

Despite the fact that the RR experiments are carried out under conditions of MAS, the RR line shapes and magnetization exchange curves show dependencies to varying degrees on the chemical shift (CS) tensor principal components, the relative orientations of the CS tensors for the two spins, the indirect spin−spin coupling constant (J_{iso}), and the zero-quantum relaxation time constant, T_2^{ZQ}.[15,16] In fact, some workers have exploited the dependence on the CS tensor orientation to solve structural problems other than distance measurements.[36,39−41,43] Our intent with the present investigation is to apply the RR experiment to a model system (phenylacetic-$^{13}C_2$ acid), which will also completely be characterized independently by the dipolar-CS method. In this fashion, it is demonstrated that the two techniques are complementary and that one method serves as a useful check on the results of the other. The importance of considering the magnitudes and orientations of shielding tensors in RR experiments has recently been emphasized by Dusold et al.[51] We examine some of the main factors that affect the precision and accuracy of the results of the RR experiment in comparison with the dipolar-CS method. In the present case, the two-dimensional spin−echo experiment[52] and ab initio calculations provide information critical to the success of the dipolar-CS technique.

To complement the experimental results, we take advantage of the considerable progress that has been made in the past decade or so in the modeling of NMR chemical shifts using ab initio techniques.[53] For example, Grant and co-workers indicate that ^{13}C chemical shielding constants in sugars can be calculated with moderate basis sets with standard deviations of about 3 ppm.[54] In the present work, the validity of using ab initio calculations to propose chemical shielding tensor magnitudes and orientations for carboxyl and methylene carbons for use in rotational resonance simulations is explored. Can ab initio methods yield estimates of these parameters at a level of accuracy that is useful in the RR simulations? What is the role of intermolecular effects in the accuracy of the calculations? In the absence of experimental shielding tensors, the results presented herein establish the advantages of applying ab initio calculations as a starting point for analyzing dipolar-recoupling experiments.

Background and Theory

(i) Dipolar-Chemical Shift NMR. Dipolar-chemical shift NMR is a useful alternative to single-crystal NMR when isolated spin pairs are of interest.[5,6] In the ideal situation, the analysis provides the principal components of the two CS tensors, the relative orientation of the CS tensors, and the effective dipolar coupling constant, R_{eff} (vide infra).[6] The two-dimensional spin−echo experiment[52] can often be used in conjunction with the dipolar-CS method to establish R_{eff}. The indirect spin−spin coupling constant (J_{iso}) can be obtained from MAS experiments. For homonuclear spin systems, there are three general cases (A_2, AX, AB), depending on the chemical shift difference between the two sites relative to the spin−spin coupling (direct and indirect) when all crystallite orientations with respect to the external applied magnetic field are considered. We treat phenylacetic-$^{13}C_2$ acid and its potassium acid salt as general AB spin systems, as the dipolar coupling constant is comparable to the chemical shift difference for at least some orientations with respect to the external applied magnetic field. The Hamiltonian for a homonuclear pair of spin-$^1/_2$ nuclei can be written as

$$\hat{H} = \hat{H}_Z + \hat{H}_{CS} + \hat{H}_D + \hat{H}_J \tag{3}$$

where the subscripts denote the Zeeman (Z), chemical shift (or chemical shielding) (CS), direct dipolar (D), and indirect spin−spin coupling (J) interactions. The total Hamiltonian gives rise to four allowed transitions[55] whose frequencies and relative intensities depend on R_{eff}, J_{iso}, the principal components of the CS tensors[56] (σ_{11}, σ_{22}, σ_{33} or, similarly, δ_{11}, δ_{22}, δ_{33}), and the relative orientations of the CS tensors. The *effective* dipolar coupling constant, mentioned above, has contributions from the direct dipolar coupling constant (eq 1) and the anisotropy in the indirect spin−spin coupling tensor, ΔJ.

$$R_{eff} = R_{DD} - \frac{\Delta J}{3} \tag{4}$$

In the present case of a carbon−carbon single bond, it is a reasonable assumption to neglect the second term in this equation. For example, $\Delta J/3$ is only 0.9% of R_{DD} in ethane.[57] In general, however, this is not always the case, especially in situations where heavier nuclei are involved and the Fermi contact interaction does not dominate the indirect spin−spin coupling tensor; the $-\Delta J/3$ term can sometimes equal or surpass R_{DD}.[58] It is also important to note that, even when it is assumed that $R_{eff} = R_{DD}$, accurate bond lengths cannot simply be derived from eq 1. This is because any dipolar coupling constant that one measures experimentally is a motionally averaged value.[4,59] Angular fluctuations as well as anharmonic stretching vibrations of the internuclear vector must be considered. Invariably, molecular motion causes a reduction in R_{DD}, and thus, the derived distance will be an upper limit.

In describing the chemical shielding and chemical shift tensors, it is advantageous to use the following conventions.[60] The principal components of the CS tensor are ordered as follows: $\sigma_{11} \leq \sigma_{22} \leq \sigma_{33}$ and, correspondingly, $\delta_{11} \geq \delta_{22} \geq \delta_{33}$. The span ($\Omega$) and the skew ($\kappa$) provide information about the shape of the powder pattern.

$$\Omega = \sigma_{33} - \sigma_{11} = \delta_{11} - \delta_{33} \tag{5}$$

$$\kappa = \frac{3(\delta_{22} - \delta_{iso})}{\Omega} \tag{6}$$

(ii) Rotational Resonance NMR. The theory of rotational resonance has been developed primarily by Levitt and co-workers.[15,17,37,45,47,61] Presented here is a brief qualitative description of the RR phenomenon essential for following the discussion presented herein. As mentioned earlier, the RR condition (eq 2) is satisfied when the MAS rate is such that, when it is multiplied by an integer, the product is equal to the difference in isotropic chemical shifts between two spins of a homonuclear spin pair. When the RR condition is fulfilled, the homonuclear dipolar interaction is partially reintroduced via the "flip-flop" term of the dipolar Hamiltonian, $\hat{H}_D$. The time-averaged dipolar Hamiltonian over one rotor period is given by[47]

$$\overline{\hbar^{-1}\hat{H}_D} = \frac{1}{2}(2\pi R_{eff})(d_n\hat{I}_{1+}\hat{I}_{2-} + d_{-n}\hat{I}_{1-}\hat{I}_{2+}) \tag{7}$$

where $n = 1, 2$. The Fourier components of the dipole−dipole coupling that depend on Euler angles defining the crystallite orientation with respect to the rotor frame are given by d_n and d_{-n}.[37,47] Thus, under RR conditions, the dipolar interaction does not average to zero over each rotor period, and hence, it will contribute to the spectrum of a MAS sample. This contribution typically manifests itself as a splitting for large values of R_{eff} and n or as a broadening for smaller values of R_{eff} and n. In theory, the line shapes depend on the CS tensors, R_{eff}, J_{iso}, and the zero-quantum relaxation time constant, T_2^{ZQ}, which describes the rate of damping of the magnetization exchange between the two spins.

Simulations of RR line shapes are a useful check to ensure that one has a spin system completely and accurately characterized.[62] In cases where R_{eff} is sufficiently large that splittings are observed in the $n = 1$ RR spectrum, line shape simulations may be suitable for determining this parameter. In the more general case, however, simulations of the longitudinal magnetization exchange curves under conditions of rotational resonance are the best approach for extracting the desired information. The experimental data are acquired by selectively inverting one of the two resonances of interest, waiting a variable mixing time, and recording the spectrum. The intensity difference, typically denoted $<\hat{I}_{z1} - \hat{I}_{z2}>$ or ρ[23], is then plotted as a function of mixing time. The resulting decay curve is simulated to obtain the available information. Approximately, these decay curves can be divided into two cases:[37,61] (i) the case of very fast dephasing (where T_2^{ZQ} is relatively short)

$$<\hat{I}_{z1} - \hat{I}_{z2}>(t) \approx \exp(-T_2^{ZQ}|\overline{\omega_B^{(n)}}|^2 t) \tag{8}$$

and (ii) the case of slow dephasing (where T_2^{ZQ} is relatively long).

$$<\hat{I}_{z1} - \hat{I}_{z2}>(t) \approx \exp(-t/2T_2^{ZQ}) \cos(|\overline{\omega_B^{(n)}}|t) \tag{9}$$

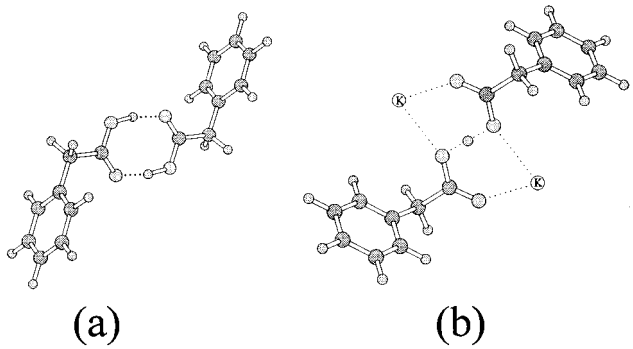

Figure 1. Dimeric structures of (a) phenylacetic acid and (b) potassium hydrogen bisphenylacetate.

Here, the $\overline{\omega_B^{(n)}}$ are the resonant Fourier components associated with the flip-flop term of the dipolar Hamiltonian for RR of order n. Note that, in the case of fast dephasing, the decay is approximately exponential, but as T_2^{ZQ} becomes larger, oscillations will become apparent.

Experimental Section

(i) Preparation of Compounds. Phenylacetic acid (98.5% purity), phenylacetic-^{13}C-*carboxy* acid (99% labeled), and phenylacetic-$^{13}C_2$-acid (99% labeled) (mp 78 °C) were obtained from Aldrich and used without further purification. Potassium hydrogen bisphenylacetate was prepared by dissolving 1 mol equiv of the acid in hot ethanol and slowly adding 1 equiv of crushed potassium hydroxide. After being stirred for 10 min, the solution was allowed to cool to room temperature and was then further cooled in a refrigerator to produce colorless needle crystals. After filtration, melting points were taken to ensure the reproducibility of the synthesis (mp 140−142 °C). It should be noted that two polymorphs, hydrates, or other related products of the reaction could also be isolated; these were observed to melt at 186−187 °C and 220−223 °C. The compound analyzed herein via NMR (mp 140−142 °C) was confirmed by single-crystal and powder X-ray diffraction to have the crystal structure reported by Bacon and co-workers[63] (see Figure 1).

For longitudinal magnetization exchange experiments, isotopically enriched samples were diluted to ∼12% by dissolving appropriate amounts of phenylacetic-$^{13}C_2$-acid (99%) and phenylacetic acid (natural abundance) in aqueous ethanol and then removing the solvent; this reduces undesirable intermolecular carbon−carbon dipolar interactions.

(ii) NMR Experiments and Analysis. Solid-state NMR experiments were carried out on Bruker AMX ($B_0 = 9.4$ T, ν_L (^{13}C) = 100.6 MHz) and Varian Chemagnetics CMX Infinity ($B_0 = 4.7$ T, ν_L (^{13}C) = 50.3 MHz) spectrometers, with high-power proton decoupling. One stationary spectrum was acquired on a home-built spectrometer (Prof. K. Zilm's laboratory, Yale University) coupled to a Tecmag Libra data system ($B_0 = 2.35$ T, ν_L (^{13}C) = 25.16 MHz). Referencing and establishment of the Hartmann−Hahn match condition for the ^{13}C NMR experiments were achieved using solid adamantane (methylene peak $\delta_{iso} = 38.57$ ppm with respect to TMS) spinning at the magic angle at a rate of 2 kHz. Although the proton relaxation times for the compounds studied herein are relatively long, recycle delays of 60−100 s resulted in spectra with excellent signal-to-noise ratios in reasonable times. Cross-polarization (CP) contact times of 0.5−5.0 ms and pulse widths of 4.0−6.0 μs were used. TPPM decoupling[64] was employed during the acquisition of the spectra of stationary samples and of most MAS samples. Two-dimensional spin−echo experiments[52] were carried out on stationary samples using the Hahn echo pulse

sequence, $\pi/2 - \tau_1 - \pi - \tau_2$. Preparation of initial conditions for the RR experiments was achieved via the DANTE[65] pulse sequence. For cases in which shielding anisotropies are relatively large, Geen et al. have proposed a more robust technique.[66]

Spectra of stationary samples were analyzed using the WSOLIDS and SpinEcho software packages, which were developed in this laboratory.[67,68] These packages incorporate the space-tiling algorithm of Alderman et al. for the efficient generation of powder patterns.[69] Simulations of the spectra of MAS samples (on and off the RR condition) were done using NMRLAB.[70] Zeeman magnetization exchange curves were simulated using the program "cc2z".[71]

(iii) Ab Initio Calculations. All calculations were carried out using Gaussian 98[72] on an IBM RISC 6000 workstation. Geometries used in the calculations were taken from the available X-ray atomic coordinates for phenylacetic acid[73] and from the neutron diffraction atomic coordinates for potassium hydrogen bisphenylacetate.[63] For the acid, carbon−hydrogen bond lengths were set to 1.09 Å.[74] Calculations on both molecules were carried out for the dimeric units shown in Figure 1. Calculations of the nuclear magnetic shielding tensors were performed using the gauge-including atomic orbitals (GIAO) method[75] at the restricted Hartree−Fock (RHF) level of theory using the 6-311G* and 6-311++G(2d,2p) basis sets[76] on all atoms. Conversion of calculated chemical shieldings to chemical shifts was done using the equation $\delta \approx \sigma_{ref} - \sigma$, where σ_{ref} is Jameson and Jameson's value for the isotropic chemical shielding for tetramethylsilane, 184.1 ppm (liquid, spherical bulb, 300 K).[77]

Results and Discussion

Because the two-dimensional spin−echo experiment[52] allows for the determination of R_{eff} with negligible dependence on CS tensors, this technique was applied to a stationary sample of phenylacetic-$^{13}C_2$ acid. This experiment yielded a value of 2110 ± 40 Hz, which was then used as a starting point in the dipolar-CS analysis. Ab initio calculations of the CS tensors (vide infra) confirm that the most shielded component of the carboxyl CS tensor lies perpendicular to the carboxyl plane. These two pieces of information are required for the dipolar-CS method to be of use in establishing the orientations of the CS tensors with respect to the molecular framework.

(i) Dipolar-Chemical Shift NMR. The relevant dipolar and CS interaction tensors in phenylacetic-$^{13}C_2$ acid and potassium hydrogen bisphenylacetate-$^{13}C_2$ were characterized via the dipolar-CS method. The X-ray crystal structure of the acid[73] and the neutron diffraction structure of the potassium acid salt[63] have been published previously; both indicate that there is only a single crystallographically distinct molecule in the unit cell. The acid exists as a hydrogen-bonded dimer. In the potassium acid salt, each phenylacetate moiety is associated with a potassium cation but also possesses an extremely short symmetric hydrogen bond to another phenylacetate anion[63] (see Figure 1). A literature search revealed no structural data for other alkali metal acid salts of phenylacetic acid.

Shown in Figure 2 are experimental spectra of a stationary powdered sample of phenylacetic-$^{13}C_2$ acid obtained at three applied magnetic fields along with the best-fit simulations. The parameters determined from the fits are reported in Table 1. A Herzfeld−Berger analysis[78] of a ^{13}C CP/MAS spectrum of a slow-spinning powdered sample of phenylacetic-^{13}C-*carboxy* acid (99%) yielded carboxyl carbon CS tensor principal components in superb agreement with those reported in Table 1. A spectrum of a stationary powdered sample of phenylacetic-

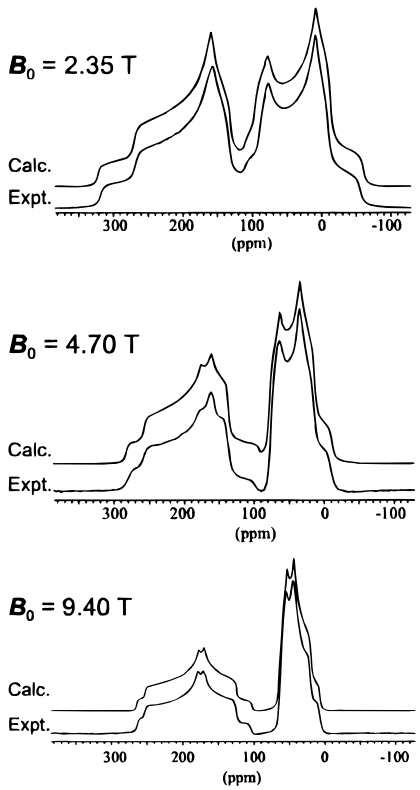

Figure 2. Carbon-13 CP NMR spectra of stationary powder samples of phenylacetic-$^{13}C_2$ acid (99%), along with best-fit simulations from the dipolar-CS method, for three different external applied magnetic fields. Number of acquisitions: 15 590 (2.35 T), 1024 (4.7 T, 9.4 T). TPPM decoupling was used for the spectra acquired at 4.7 and 9.4 T. Recycle delays: 20 s (2.35 T), 60 s (4.7 T, 9.4 T). Best-fit parameters are given in Table 1.

TABLE 1: Dipolar-Chemical Shift Results for Phenylacetic-$^{13}C_2$ Acid and Potassium Hydrogen Bisphenylacetate-$^{13}C_2$

	phenylacetic acid		potassium hydrogen bisphenylacetate	
	^{13}CO	$^{13}CH_2$	^{13}CO	$^{13}CH_2$
δ_{11}/ppm	256.0 ± 1.0	55.0 ± 0.5	253.0 ± 1.5	56.5 ± 1.0
δ_{22}/ppm	176.0 ± 1.5	50.5 ± 1.0	184.0 ± 1.0	50.0 ± 1.0
δ_{33}/ppm	111.5 ± 1.5	20.0 ± 0.5	108.0 ± 1.0	32.5 ± 1.5
δ_{iso}/ppm	181.2	41.8	181.3	46.3
Ω/ppm	144.5	35.0	132.5	24.0
κ	−0.107	0.743	0.200	0.458
α^a	10.0° ± 4.0°	0.0° ± 4.0°	0.0[b]	0.0[b]
β	90.0° ± 4.0°	42.0° ± 1.0°	90.0 ± 5.0°	0.0 ± 6.0°
γ	42.5° ± 1.0°	100.0° ± 5.0°	31.5 ± 1.5°	0.0 ± 20.0°
R_{eff}/Hz	2150 ± 30		2060 ± 50	

[a] α, β, and γ are Euler angles relating the CS tensors to the dipolar tensor. See ref 62 for a discussion of the definition of Euler angles used here. [b] Powder patterns were observed to be insensitive to variations in this parameter; a value of 0.0 was used in the simulations.

^{13}C-*carboxy* acid (99%) also gave tensor components in agreement with those reported in Table 1. It has been shown in the past[6,62] and will be re-emphasized here that the reliability of dipolar-CS results depends strongly on having acquired spectra at more than one external applied magnetic field strength. We have acquired stationary spectra at 2.35, 4.70, and 9.40 T. Continuous-wave (CW) decoupling (~70 kHz) was not sufficient to completely resolve the spectral features in the methylene region at 4.70 and 9.40 T. Two-pulse phase-modulated (TPPM) decoupling[64] was employed. The spectra for potassium hydrogen bisphenylacetate-$^{13}C_2$, obtained at 4.7 and

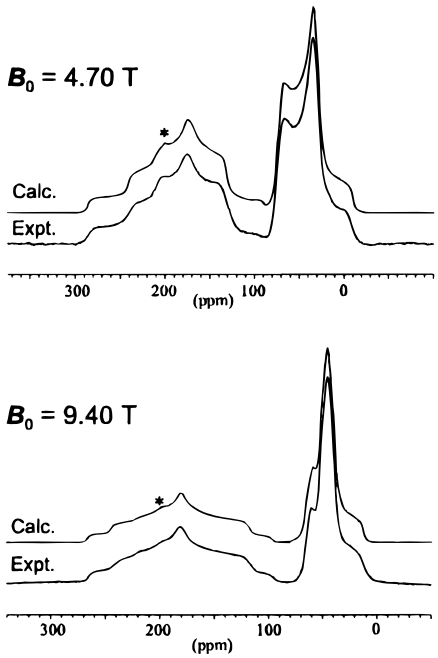

Figure 3. Carbon-13 CP/TPPM NMR spectra of stationary powder samples of potassium hydrogen bisphenylacetate-$^{13}C_2$ (99%), along with best-fit simulations from the dipolar-CS method, for two different external applied magnetic fields. Number of acquisitions: 1024. Recycle delay: 60 s. Best-fit parameters are given in Table 1. Asterisks indicate features attributed to an impurity (see text).

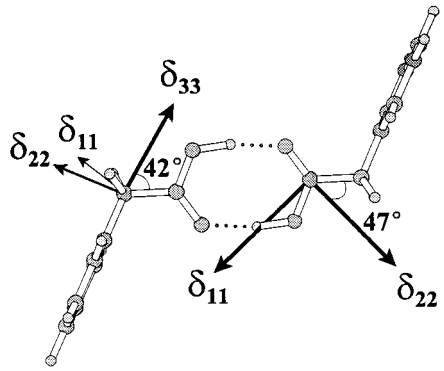

Figure 4. Experimental orientations of the methylene and carboxyl carbon CS tensors with respect to the molecular frame for phenylacetic acid. See Table 1 for Euler angles relating the CS tensors to the dipolar tensor and for the CS tensor principal components. The phenyl rings are perpendicular to the plane of the page. The tensors on each half of the dimer are related by an inversion center. For clarity, the methylene tensor is shown on one half and the carboxyl tensor is shown on the other half. For the carboxyl carbon, the direction of greatest shielding is perpendicular to the plane of the page. For the methylene carbon, the direction of greatest shielding is in the plane of the page.

9.4 T, and best-fit simulations are presented in Figure 3. The parameters determined from the fits are given in Table 1.

One of the shoulders in the spectra of the labeled potassium acid salt, marked with an asterisk in Figure 3, does not arise from the best-fit parameters and is not attributed to potassium hydrogen bisphenylacetate. Rather, we ascribe this shoulder to one of the other reaction products (mp ~186 °C) present in a proportion of 10−15% relative to potassium hydrogen bisphenylacetate. This was confirmed by fitting spectra of the minor product at two applied fields (spectra not shown). It should be noted that addition of 10−15% of this impurity did not notably alter any other region of the spectrum aside from the shoulder indicated; in fact, its effect even at this shoulder is hardly noticeable at 9.4 T. For the remainder of this discussion, we will only refer to the major product, potassium hydrogen bisphenylacetate.

In accord with the findings of Gu and McDermott,[10] our results show that, upon moving from the acid to the acid salt, the least shielded component of the carboxyl carbon shift tensor, δ_{11}, decreases, while δ_{22} increases. Note that the variations in the principal components almost cancel one another; the difference in the isotropic chemical shifts of the carboxyl carbons in the acid and the potassium acid salt is less than 1 ppm. This fact emphasizes the importance of studying NMR interaction *tensors* rather than their isotropic values. Another measure of the effect of the protonation state on the carboxyl CS tensor is the change in its span, Ω, and skew, κ. In the potassium acid salt, Ω is observed to decrease by 12 ppm; a decrease in the span is perhaps intuitive given the fact that complete deprotonation would render the two oxygen atoms more similar to each other by virtue of delocalization of the lone pair of electrons over both oxygen atoms. The skew is observed to change sign, from negative to positive, upon moving from the acid to the acid salt. These results are supported by ab initio calculations (vide infra). Facelli and co-workers have examined the dependence of the carboxyl shielding tensor on the strength of the hydrogen bond in acetic acid.[79] Their results indicate that the difference between δ_{11} and δ_{22} is an indicator of the relative delocalization of the π electrons of the carbonyl group, the strength of the hydrogen bond, and the geometry of the carboxyl group.

The CS tensors of methylene carbons have not been as extensively studied as those of carboxyl carbons.[7−9] For the methylene carbon, the tensorial nature of chemical shielding is again evident (Table 1). Although the isotropic chemical shift difference between the potassium acid salt and the acid is only ~4 ppm, the most shielded component (δ_{33}) increases by 12.5 ppm upon moving from the acid to the acid salt. As a result, the span of the methylene carbon CS tensor decreases from 35 ppm in the acid to 24 ppm in the potassium acid salt. Additionally, κ changes significantly for the methylene carbon shielding tensor, which is not evident from Figures 2 and 3 because the dipolar splittings are comparable to the span (in hertz). Hydrogen bonding is known to be very important in carboxylic acids and carboxylates;[11,80−83] these effects, along with accompanying changes in bond lengths and bond angles, are responsible for the observed changes in the CS tensors in the carboxyl and methylene carbons. The results obtained here can be compared with the methylene shielding tensor data reported by Jagannathan for malonic acid (Ω = 44 ppm, κ = 0.48) and succinic acid (Ω = 44 ppm, κ = 0.41).[9b]

The experimental orientations of the CS tensors are depicted in Figures 4−6. Euler angles defining the experimental orientations are given in Table 1. In the case of carboxyl carbons in carboxylic acids, it is well-known that the most shielded component is approximately perpendicular to the COO plane and that the intermediate component lies roughly along the C═O bond.[9a,10−13] Thus, for the experimental orientations, the assumption is made that δ_{33} is exactly perpendicular to the carboxyl plane; this assumption is supported by ab initio calculations (vide infra). With this established, it is also possible to determine the orientation of the methylene carbon CS tensor with respect to the molecular frame. Referring to the carboxyl carbon, it is evident that, upon moving from phenylacetic acid to potassium hydrogen bisphenylacetate, the intermediate component, δ_{22}, remains approximately along the shorter of the two carbon−oxygen bonds. In the acid, this is the carbonyl group. It should be noted that, for both the acid and the acid salt, there

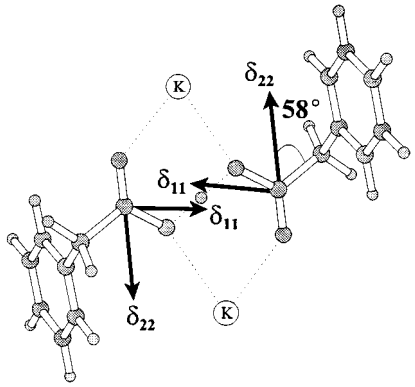

Figure 5. Experimental orientation of the carbonyl carbon CS tensor with respect to the molecular frame for potassium hydrogen bisphenylacetate. See Table 1 for Euler angles relating this tensor to the dipolar tensor and for the CS tensor principal components. The direction of greatest shielding is perpendicular to the plane of the page. The intermediate component, δ_{22}, lies along the shorter of the two carbon−oxygen bonds.

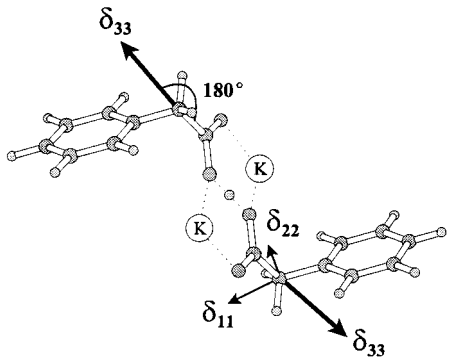

Figure 6. Experimental orientation of the methylene carbon CS tensor with respect to the molecular frame for potassium hydrogen bisphenylacetate. See Table 1 for Euler angles relating this tensor to the dipolar tensor and for the CS tensor principal components. Experimentally, it was not possible to fix the direction of the δ_{11} and δ_{22} components. Shown here is the orientation of these components predicted by ab initio calculations at the RHF/6-311++G(2d,2p) level.

are two possible orientations for the δ_{11} and δ_{22} components that arise from the dipolar-chemical shift analysis. The choice supported by the ab initio orientations is represented in Figures 4 and 5. The other possibility results from a rotation of δ_{11} and δ_{22} through 180° about an axis passing through the carboxyl−methylene carbon−carbon bond. Consequently, this rotation would place the δ_{22} component approximately along the longer carbon−oxygen bond in both the acid and the potassium acid salt.

Perhaps more interesting is the effect of the protonation state on the methylene carbon CS tensor; not only is this atom further removed from the hydroxyl group, but symmetry does not dictate the direction of any of its principal components as is the case for carboxyl carbon CS tensors. Schmidt−Rohr and Spiess note that, for $X-CH_2-Y$ groups, the δ_{11} component is predicted to be orthogonal to the approximate local mirror plane bisecting the H−C−H bond.[84] In his single-crystal NMR analysis of the carbon shielding tensors in *n*-$C_{20}H_{42}$, VanderHart finds that the δ_{22} component of the interior methylene shielding tensor bisects the H−C−H angle, but concludes that, in general, crystal packing forces and anisotropic motion of the atoms will significantly affect the observed methylene CS tensors.[8a] In the cases of phenylacetic acid and its potassium acid salt, a prediction of the orientations of the methylene CS tensors based on local symmetry does not seem feasible because of the marked difference in the nature of the two groups bonded to the $-CH_2-$ fragment. As is apparent in Figure 4, the most shielded component lies approximately in line with the $H_2\underline{C}-$ ipso carbon bond in the acid. In the acid salt, however, the orientation changes such that δ_{33} is along the carboxyl−methylene carbon−carbon bond (Figure 6). As noted in Table 1, the appearance of the spectra of the potassium acid salt was invariant to changes in the Euler angle α. This implies that, whereas the δ_{33} component of the methylene CS tensor is fixed along the carbon−carbon bond of the H_2C-COO fragment, the δ_{11} and δ_{22} components can lie anywhere in the plane that they define. This lack of orientation dependence of the spectrum arises from the small span of the methylene shielding tensor. The orientations of the δ_{11} and δ_{22} components shown in Figure 6 are taken from the ab initio results.

The other important piece of information that is refined within the dipolar-CS experiment is the effective dipolar coupling constant, R_{eff} (see eqs 1 and 4). The determination of the dipolar coupling constant via the dipolar-chemical shift method relies on the assumption that δ_{33} is exactly perpendicular to the carboxyl plane. As shown in Table 1, R_{eff} was determined to be 2150 ± 30 Hz for phenylacetic acid and 2060 ± 50 Hz for its potassium acid salt. If we assume a negligible anisotropy in the carbon−carbon indirect spin−spin coupling tensor, $\Delta J = 0$, then the reduction in R_{DD} due to molecular motion can be calculated with knowledge of the crystal structure data. We calculate $R_{\text{DD}} = 2283$ Hz for the acid, using a bond length of 1.493 Å.[73] Motional averaging thus causes a reduction of about 6% in R_{DD}; the reduction in potassium hydrogen bisphenylacetate is also 6%. The neutron diffraction study of the potassium acid salt[63] reports large anisotropic motions of the methylene group, as well as the aromatic carbons (and directly bonded protons) meta and para to the ipso carbon. This motion is responsible, in part, for the reduction in the direct dipolar coupling constant.

(ii) Ab Initio Calculations. The results of the ab initio GIAO shielding calculations for dimeric phenylacetic acid and potassium hydrogen bisphenylacetate (Figure 1) at the RHF/6-311G* and RHF/6-311++G(2d,2p) levels are summarized in Table 2. Overall, the agreement between the experimental and ab initio results is quite good. For both the acid and the acid salt, increasing the size of the basis set by including more polarization functions and diffuse functions marginally improves the agreement between experiment and theory. Both calculations successfully predict the sign of the skews of both the carboxyl and methylene shielding tensors. In addition, both the isotropic chemical shifts and spans are in qualitative agreement with the experimental results. Despite the ability of the calculations to provide some useful information, quantitative agreement between experiment and theory is lacking. For example, isotropic chemical shifts are in error by over 10 ppm for the methylene carbons, and the spans of the carboxyl carbons are consistently overestimated. Despite our efforts to account for an intermolecular contribution to the shielding by carrying out these calculations on dimeric units, it is certain that other nearest-neighbor molecules will also contribute.[85] Additionally, ^{13}C chemical shifts are known to increase upon moving from the gas phase to a condensed phase;[86] thus, it is expected that high-level ab initio calculations, which are for isolated molecules (or dimers) in the gas phase, will generally yield results that are too shielded.

The calculated orientations of the carboxyl shielding tensors for both molecules are in excellent agreement with experiment. The calculations predict that δ_{33} is perpendicular to the carboxyl plane, and the predicted orientations of the δ_{11} and δ_{22}

TABLE 2: Comparison of Calculated and Experimental Chemical Shift Tensors[a] for the Carboxyl and Methylene Carbon Atoms in the Dimers of Phenylacetic Acid and Its Potassium Acid Salt[b]

		carboxyl			methylene		
compound	method	δ_{iso}/ppm	Ω/ppm	κ	δ_{iso}/ppm	Ω/ppm	κ
acid dimer	RHF/6-311G*	169.8	169.2	−0.10	24.2	45.3	0.81
	RHF/6-311++G(2d,2p)	172.6	168.0	−0.08	25.7	45.6	0.80
	experiment	181.2	144.5	−0.11	41.8	35.0	0.74
acid salt dimer	RHF/6-311G*	174.9	174.2	0.08	31.8	20.1	0.53
	RHF/6-311++G(2d,2p)	178.0	171.6	0.11	33.1	19.9	0.55
	experiment	181.3	132.5	0.20	46.3	24.0	0.46

[a] Calculated orientations of the chemical shift tensors are discussed in the text. [b] See Figure 1.

components are within 1° of the experimental orientations shown in Figures 4 and 5. These calculated orientations were essentially identical for both basis sets. Also, computations on the isolated phenylacetic acid monomer did not give a significantly different result for the orientation of the carboxyl shielding tensor. The calculations indicate that hydrogen bonding stabilizes the acid dimer with respect to the monomer by approximately 100 kJ mol^{-1}.

For the orientations of the methylene carbon shielding tensors, the calculations offer respectable results, especially given the relatively small orientation dependence of the shielding for these atoms (e.g., the span of the methylene carbon shielding tensor in the acid salt is only 24 ppm). For the acid, the direction of δ_{33} with respect to the carboxyl−methylene carbon internuclear vector is within 1° of the orientation shown in Figure 4. In the acid salt, calculations [RHF/6-311++G(2d,2p)] indicate that δ_{33} is approximately 13° away from the carboxyl−methylene carbon internuclear vector; the experimental result (Figure 6) predicts collinearity of δ_{33} and the internuclear vector. Experimentally, rotation of the methylene shielding tensor in the acid salt about the most shielded component led to no observable changes in the simulated spectra. The calculated orientation of these components is shown in Figure 6, with δ_{11} approximately in the plane of the phenyl ring.

(iii) Rotational Resonance NMR. Having characterized the CS and direct dipolar coupling tensors for the methylene-carboxyl carbon spin pair in phenylacetic-$^{13}C_2$ acid and its potassium acid salt, we now demonstrate that the RR technique can be employed to complement our results and to determine the sensitivity of the RR results to various parameters and experimental conditions.

Shown in Figures 7−10 are experimental and calculated spectra of MAS samples of phenylacetic-$^{13}C_2$ acid and its potassium acid salt. In the case where the RR condition is not satisfied, there is no splitting or broadening of the individual resonances. For the $n = 1$, $n = 2$, and $n = 3$ RR conditions, however, the effects of the homonuclear dipolar interaction are clearly evident. The simulated spectra employ the parameters determined from the dipolar-CS method (Table 1). The agreement between the observed RR line shapes and the line shapes calculated from the dipolar-CS parameters is excellent. We note here a complication encountered in attempting to simulate the RR line shapes shown in Figures 7−10. Although the dipolar and CS tensor information obtained from the dipolar-CS method is accurate, satisfactory fits were initially difficult to obtain. A critical factor in fitting the higher-order RR spectra ($n = 2$, 3) was the MAS rate used in the simulation. To demonstrate this dependence, we have simulated a series of $n = 3$ RR MAS spectra for the carboxyl carbon in zinc acetate-$^{13}C_2$ (Figure 11); this compound was employed in setting up our RR experiments because it has been previously analyzed by rotational resonance NMR.[15] As illustrated, the $n = 3$ line shape is extremely dependent on the MAS rate. Two experimental spectra for zinc

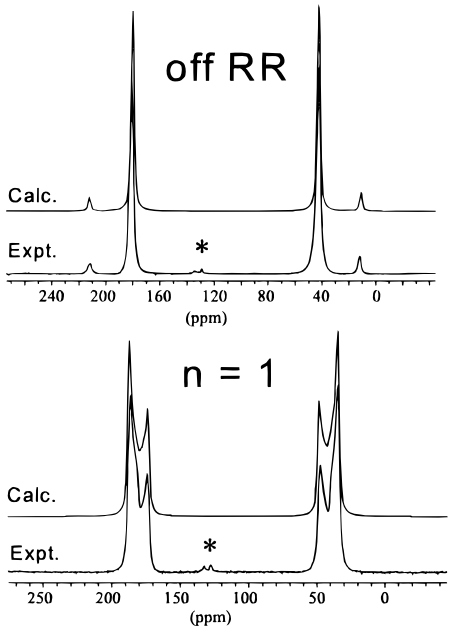

Figure 7. Off-RR and $n = 1$ RR ^{13}C CP/MAS spectra of phenylacetic-$^{13}C_2$ acid (99%). $B_0 = 4.7$ T, $\nu_L = 50.3$ MHz, number of acquisitions = 256. The "off-RR" spectrum was acquired with variable-amplitude CP, $\nu_{rot} = 9.0$ kHz. Signal due to naturally abundant ^{13}C in the phenyl ring is indicated by asterisks.

acetate-$^{13}C_2$ shown in reference 35 for the $n = 3$ RR condition seem to be inconsistent with each other; a slight difference in the MAS rate resolves this apparent discrepancy. Thus, it is extremely important to have a stable, accurate MAS rate in the RR experiment and to optimize this rate in the simulations in order to ensure appropriate fits.

It is obvious in Figures 7−10 that, despite the marked differences in the CS tensors of the acid and the acid salt, their RR line shapes are strikingly similar. Comparable line shapes were also observed for the rubidium salt of phenylacetic acid. Thus, an accurate determination of the CS tensor principal components and orientations using RR spectra does not seem feasible. These line shapes are sensitive to the dipolar coupling constant, however. Accordingly, these RR spectra can rapidly provide a rough estimate of the dipolar coupling constant. A problem with this method, however, concerns the fact that, if large distances are to be determined (i.e., a few angstroms or more), then even the $n = 1$ RR spectrum becomes broadened rather than distinctly split; this makes accurate determinations of R_{eff} more difficult. We note that any discrepancies in the RR spectra of the potassium acid salt are likely attributable to the 10−15% impurity that was not incorporated into these simulations. Additionally, problems associated with residual heteronuclear couplings recently described by Helmle et al.[45] could contribute to the experimental MAS line shapes for both the acid and the potassium acid salt.

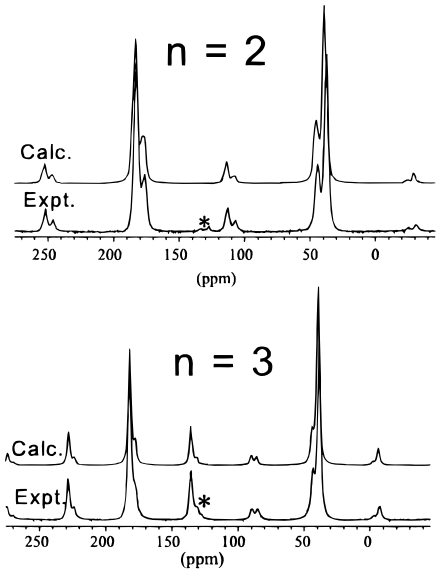

Figure 8. Rotational resonance ($n = 2$ and $n = 3$) ^{13}C CP/MAS spectra of phenylacetic-$^{13}C_2$ acid (99%). $B_0 = 4.7$ T, $\nu_L = 50.3$ MHz, number of acquisitions = 256. Signal due to naturally abundant ^{13}C in the phenyl ring is indicated by asterisks.

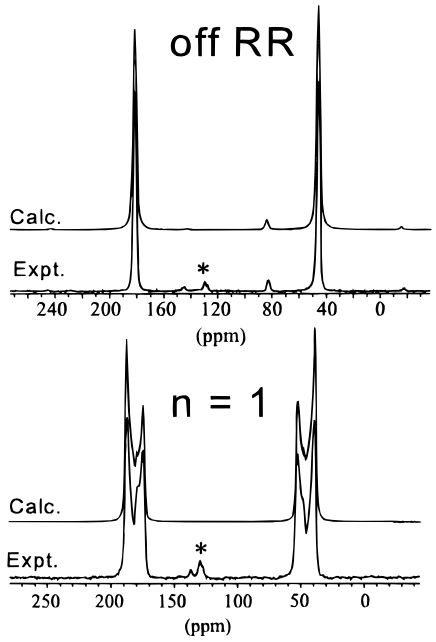

Figure 9. Off-RR and $n = 1$ RR ^{13}C CP/MAS spectra of potassium hydrogen bisphenylacetate-$^{13}C_2$ (99%). $B_0 = 4.7$ T, $\nu_L = 50.3$ MHz, number of acquisitions = 64. The "off-RR" spectrum was acquired with variable-amplitude CP, $\nu_{rot} = 9.0$ kHz. Signal due to naturally abundant ^{13}C in the phenyl ring is indicated by asterisks.

More commonly than the above-mentioned MAS spectral simulations, longitudinal magnetization exchange curves have been used to extract information about homonuclear spin systems. Shown in Figures 12 and 13 are the $n = 1$ and $n = 2$ exchange curves for phenylacetic-$^{13}C_2$ acid (diluted to ~12% enrichment), along with the best-fit simulations. As the order of the rotational resonance increases, it is known that the CS tensors play an increasingly important role in determining the shape of the exchange curve.[15−17] Thus, the $n = 1$ curve is essentially a damped cosine curve (obeying eq 9 more so than eq 8), and R_{eff} can easily be determined without knowledge of the CS tensors. To obtain a satisfactory fit to the experimental data over the time scale shown, however, the CS tensor

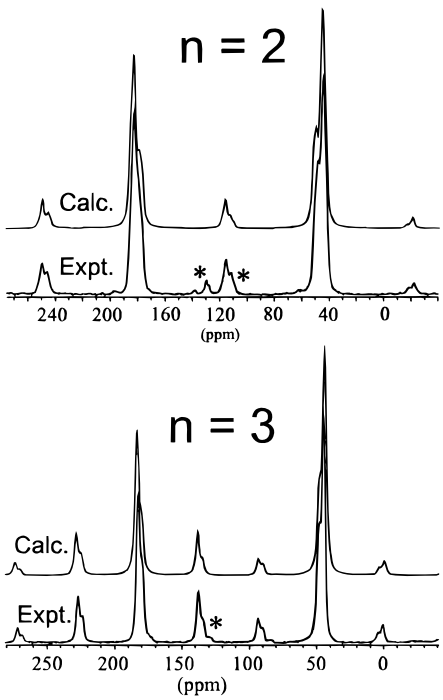

Figure 10. Rotational resonance ($n = 2$ and $n = 3$) ^{13}C CP/MAS spectra of potassium hydrogen bisphenylacetate-$^{13}C_2$ (99%). $B_0 = 4.7$ T, $\nu_L = 50.3$ MHz, number of acquisitions = 256. Signals due to naturally abundant ^{13}C in the phenyl ring are indicated by asterisks.

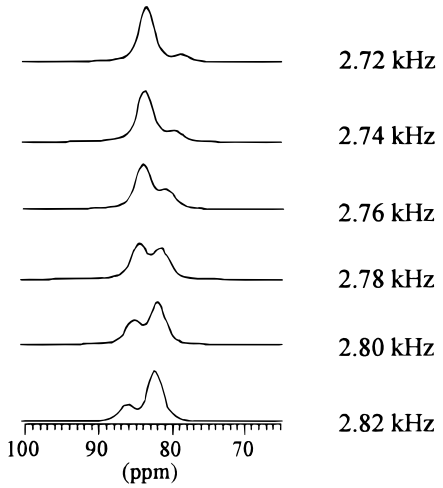

Figure 11. Simulated ^{13}C spectra for the carboxyl carbon in zinc acetate-$^{13}C_2$ at a range of MAS rates near the $n = 3$ RR condition. $B_0 = 4.7$ T. Note the marked dependence of the line shape on MAS rate.

orientations obtained from the dipolar-CS method were found to be essential even for the $n = 1$ case. The zero-quantum relaxation time constant, T_2^{ZQ}, is also required if one wishes to obtain proper fits. In our simulations, this parameter was simply optimized; for phenylacetic-$^{13}C_2$ acid, a value of $T_2^{ZQ} = 12.0$ ms was used. Because J_{iso} is known to be small relative to the dipolar coupling constant for carbon−carbon single bonds (~2%), the effect of the former is not noticeable (the value obtained from a solution ^{13}C NMR spectrum is 53 Hz; similar values have been obtained for a series of carboxylate esters[87]). However, for ^{31}P spin pairs, for example, J_{iso} is yet another variable that must be taken into account in the simulations.[62] The effective dipolar coupling constant determined from the $n = 1$ exchange curve, $R_{eff} = 2100 \pm 15$ Hz, is in very good agreement with the result obtained from the dipolar-CS method ($R_{eff} = 2150 \pm 30$ Hz). The RR datum thus seems to indicate

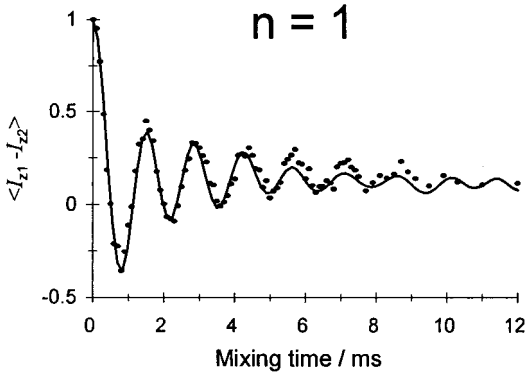

Figure 12. Normalized $n = 1$ RR longitudinal magnetization exchange curve for phenylacetic-$^{13}C_2$ acid (diluted to ~12% enrichment). The DANTE sequence was used to prepare the initial conditions. Sixteen scans were acquired for each experimental point with a recycle delay of 60 s; $\langle \hat{I}_{z1} - \hat{I}_{z2} \rangle$ values were determined by integration and then normalized with respect to zero mixing time. $B_0 = 4.7$ T.

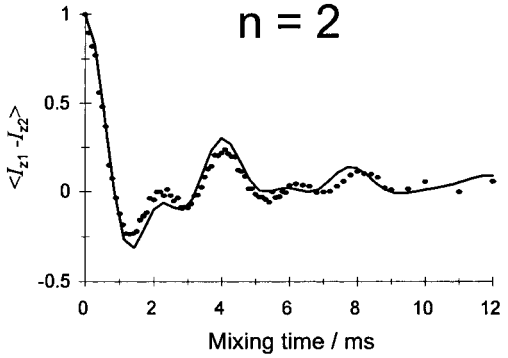

Figure 13. Normalized $n = 2$ RR longitudinal magnetization exchange curve for phenylacetic-$^{13}C_2$ acid (diluted to ~12% enrichment). The DANTE sequence was used to prepare the initial conditions. Sixteen scans were acquired for each experimental point with a recycle delay of 60 s; $\langle \hat{I}_{z1} - \hat{I}_{z2} \rangle$ values were determined by integration and then normalized with respect to zero mixing time. $B_0 = 4.7$ T.

a slightly greater degree of motional averaging of R_{DD} than for the dipolar-CS method. For the $n = 2$ exchange curve, the orientations of the CS tensors were imperative for producing an acceptable simulation. Calculation of the carbon−carbon bond length directly from the effective dipolar coupling constant gives $r_{CC} = 1.535$ Å from the RR experiment; from the X-ray structure, $r_{CC} = 1.493(4)$ Å. These results are in very good agreement considering that the NMR result is a motionally averaged value.

Presented in Figure 14 is series of simulated exchange curves for phenylacetic-$^{13}C_2$ acid, demonstrating the dependence of the $n = 1$ curve on the magnitude of the dipolar coupling constant. The various simulations differ in that the effective dipolar coupling constant has been incremented by 50 Hz, from 1900 to 2200 Hz. From these results, one can see that the dipolar coupling constant can be easily determined to within less than 50 Hz using the $n = 1$ curve. This corresponds to a precision of about 0.04 Å, which is the difference between the distances derived from the RR experiment and from the X-ray structure for the acid. The curves in Figure 15 demonstrate the dependence of the $n = 2$ exchange curve on the carboxyl carbon Euler angle γ, which describes the rotation of the CS tensor about the direction perpendicular to the carboxyl plane. The best-fit value, $\gamma = 42.5°$, is represented, along with comparable values of 30.0° and 50.0°. Clearly, these exchange curves are quite sensitive to the dipolar coupling constant and to changes in the

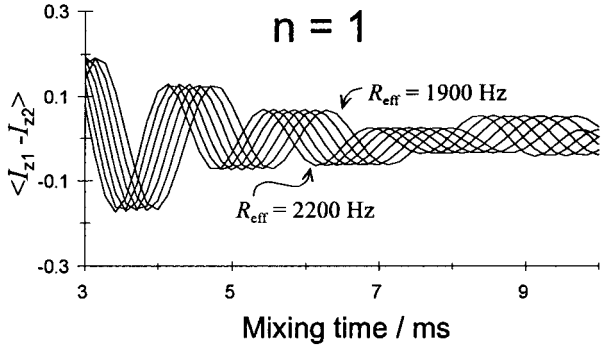

Figure 14. Simulated $n = 1$ RR exchange curves for the carboxyl−methylene isolated spin pair in phenylacetic acid. This plot illustrates the sensitivity of the $n = 1$ exchange to the value of the effective dipolar coupling constant. Each curve differs in R_{eff} by 50 Hz from the adjacent curve.

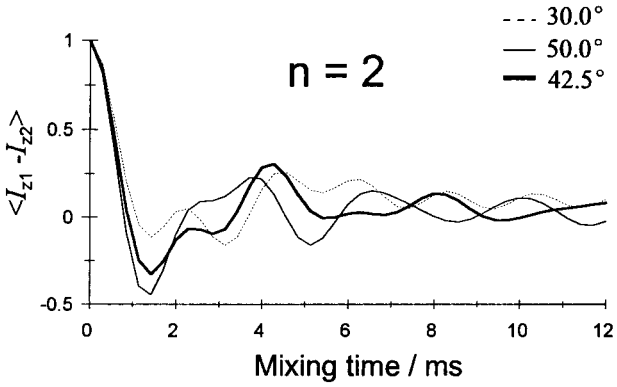

Figure 15. Simulated $n = 2$ RR exchange curves for the carboxyl−methylene isolated spin pair in phenylacetic acid. This plot demonstrates the sensitivity of the $n = 2$ exchange to the carboxyl carbon CS tensor Euler angle γ; this angle represents the rotation of the tensor about the direction perpendicular to the COO plane.

relative orientations of the CS tensors. This sensitivity further confirms the accuracy and precision of the parameters reported in Table 1.

Phenylacetic-$^{13}C_2$ acid is readily available commercially; it is relatively inexpensive; its X-ray crystal structure is in the literature;[73] and, as a result of the present work, the relevant CS and dipolar tensors have been accurately and precisely characterized both by dipolar-chemical shift and rotational resonance NMR techniques. Zinc acetate-$^{13}C_2$, which has been used in the past as a setup sample for rotational resonance experiments, is not readily available commercially and may exist in both anhydrous[88] and dihydrated forms.[89] Additionally, the orientations of the CS tensors of the carbonyl and methyl carbons in zinc acetate have not, to our knowledge, been characterized independently of the RR experiment. The tensor orientations have usually been assumed[37] on the basis of common features of carbon shift tensors outlined by Mehring.[90] Hence, we recommend phenylacetic-$^{13}C_2$ acid as a setup sample for ^{13}C rotational resonance and other homonuclear recoupling experiments.

Conclusions

The present investigation has focused on the carboxyl−methylene carbon homonuclear spin pair in phenylacetic acid and potassium hydrogen bisphenylacetate. The dipolar-chemical shift method illustrates quite clearly the effects of the protonation state of phenylacetic acid on both the magnitudes and relative orientations of the CS tensors for both the carboxyl and

methylene carbons. Definite changes in the span, skew, and orientations have been revealed. The orientation of the methylene carbon CS tensor changes significantly even though it is two atoms removed from the site of deprotonation. Ab initio calculations of the CS tensors are in very good accord with the experimental results. In fact, in the absence of experimental data, the ab initio results presented herein offer an excellent starting point for RR simulations. For other compounds to be examined via RR, such calculations (perhaps on model compounds) should prove to be beneficial, thus circumventing the necessity to assume tensor orientations in RR simulations.

By applying both the dipolar-chemical shift and rotational resonance NMR methods to phenylacetic acid and its potassium acid salt, we find that these two methods are complementary if one is interested in characterizing both the CS tensors and the effective dipolar coupling constant. Although the effective dipolar coupling constant can be extracted with reasonable reliability in the absence of accurate CS tensor information from $n = 1$ RR longitudinal magnetization exchange curves, and perhaps even from the $n = 1$ MAS line shape, the most accurate results are obtained when information about the CS tensors is known. The dependence of the exchange curves on tensor orientation and dipolar coupling has been demonstrated. The precision of the dipolar coupling constants determined from the two techniques are comparable. The primary advantage of the RR technique clearly lies in the $n = 1$ case, for which the CS tensor orientations are relatively unimportant. Provided that dependable assumptions about the CS tensors can be made, accurate internuclear distances can be determined. For the higher-order rotational resonances, however, great caution should be exercised if the CS tensors are not known. To extract R_{eff} from dipolar-CS NMR spectra, the orientation of one of the principal components of one of the CS tensors must be dictated by local symmetry; dipolar splittings must also be observed for this method to be useful. We suggest phenylacetic-$^{13}C_2$ acid as a setup sample for ^{13}C rotational resonance NMR and other homonuclear dipolar recoupling experiments.

Acknowledgment. The authors thank the members of the solid-state NMR group at Dalhousie University for many helpful comments. We also thank Prof. Glenn Penner, Prof. Gang Wu, and Dr. Scott Kroeker for contributing to the early stages of this project. We are also especially grateful to Dr. Klaus Eichele for many helpful discussions. We thank Professor T. S. Cameron and Dr. James F. Britten for X-ray analyses of potassium hydrogen bisphenylacetate. We acknowledge Dr. B. Q. Sun and Prof. R. G. Griffin for use of their simulation program NMRLAB and Dr. Y. K. Lee and Prof. M. H. Levitt for use of their simulation program cc2z. R.E.W. thanks NSERC (Canada) for a major installation grant to purchase a new console for our 4.7 T magnet and for a research (operating) grant. D.L.B. is grateful to NSERC and to the Izaak Walton Killam Trust for postgraduate scholarships. The ^{13}C NMR spectra at 2.35 T were acquired in Prof. K. Zilm's laboratory at Yale University by Dr. Sean Burns and Dr. Anil Mehta. All other spectra were obtained at the Atlantic Region Magnetic Resonance Centre, which is also supported by NSERC.

References and Notes

(1) VanderHart, D. L.; Gutowsky, H. S. *J. Chem. Phys.* **1968**, *49*, 261.
(2) VanderHart, D. L.; Gutowsky, H. S.; Farrar, T. C. *J. Chem. Phys.* **1969**, *50*, 1058.
(3) Linder, M.; Höhener, A.; Ernst, R. R. *J. Chem. Phys.* **1980**, *73*, 4959.
(4) Zilm, K. W.; Grant, D. M. *J. Am. Chem. Soc.* **1981**, *103*, 2913.
(5) Wasylishen, R. E.; Curtis, R. D.; Eichele, K.; Lumsden, M. D.; Penner, G. H.; Power, W. P.; Wu, G. In *Nuclear Magnetic Shieldings and Molecular Structure*; Tossell, J. A., Ed.; NATO Series C: Mathematical and Physical Sciences; Kluwer Academic Publishers: Dordrecht, Germany, 1993; Vol. 386, pp 297−314.
(6) Eichele, K.; Wasylishen, R. E. *J. Magn. Reson. A* **1994**, *106*, 46.
(7) Duncan, T. M. *Principal Components of Chemical Shift Tensors: A Compilation*, 2nd ed.; The Farragut Press: Chicago, IL, 1994.
(8) (a) For a single-crystal NMR characterization of a methylene carbon shielding tensor, see: VanderHart, D. L. *J. Chem. Phys.* **1976**, *64*, 830. (b) For an example of anisotropic shielding for a peptide α-carbon, see: Heller, J.; Laws, D. D.; Tomaselli, M.; King, D. S.; Wemmer, D. E.; Pines, A.; Havlin, R. H.; Oldfield, E. *J. Am. Chem. Soc.* **1997**, *119*, 7827.
(9) (a) Veeman, W. S. *Prog. Nucl. Magn. Reson. Spectrosc.* **1984**, *16*, 193. (b) Jagannathan, N. R. *Magn. Reson. Chem.* **1989**, *27*, 941.
(10) Gu, Z.; McDermott, A. *J. Am. Chem. Soc.* **1993**, *115*, 4282.
(11) van Dongen Torman, J.; Veeman, W. S.; de Boer, E. *Chem. Phys.* **1977**, *24*, 45.
(12) (a) Kempf, J.; Spiess, H. W.; Haeberlen, U.; Zimmermann, H. *Chem. Phys. Lett.* **1972**, *17*, 39. (b) Kempf, J.; Spiess, H. W.; Haeberlen, U.; Zimmermann, H. *Chem. Phys.* **1974**, *4*, 269.
(13) Nagaoka, S.; Terao, T.; Imashiro, F.; Saika, A.; Hirota, N.; Hayashi, S. *Chem. Phys. Lett.* **1981**, *80*, 580.
(14) Andrew, E. R.; Bradbury, A.; Eades, R. G.; Wynn, V. T. *Phys. Lett.* **1963**, *4*, 99.
(15) Raleigh, D. P.; Levitt, M. H.; Griffin, R. G. *Chem. Phys. Lett.* **1988**, *146*, 71.
(16) Bryce, D. L.; Wasylishen, R. E. In *Encyclopedia of Spectroscopy and Spectrometry*; Lindon, J. C., Tranter, G. E., Holmes, J. L., Eds.; Academic Press Ltd.: London, 2000; pp 2136−2144.
(17) Karlsson, T. Ph.D. Thesis, Stockholm University, Stockholm, Sweden, 1999.
(18) Tycko, R.; Dabbagh, G. *J. Am. Chem. Soc.* **1991**, *113*, 9444.
(19) Gullion, T.; Vega, S. *Chem. Phys. Lett.* **1992**, *194*, 423.
(20) Bennett, A. E.; Ok, J. H.; Griffin, R. G., Vega, S. *J. Chem. Phys.* **1992**, *96*, 8624.
(21) Fujiwara, T.; Ramamoorthy, A.; Nagayama, K.; Hioka, K.; Fujito, T. *Chem. Phys. Lett.* **1993**, *212*, 81.
(22) Joers, J. M.; Rosanske, R.; Gullion, T.; Garbow, J. R. *J. Magn. Reson. A* **1994**, *106*, 123.
(23) Nielsen, N. C.; Bildsøe, H.; Jakobsen, H. J.; Levitt, M. H. *J. Chem. Phys.* **1994**, *101*, 1805.
(24) Sun, B.-Q.; Costa, P. R.; Kocisko, D.; Lansbury, P. T., Jr.; Griffin, R. G. *J. Chem. Phys.* **1995**, *102*, 702.
(25) Takegoshi, K.; Nomura, K.; Terao, T. *Chem. Phys. Lett.* **1995**, *232*, 424.
(26) Lee, Y. K.; Kurur, N. D.; Helmle, M.; Johannessen, O. G.; Nielsen, N. C.; Levitt, M. H. *Chem. Phys. Lett.* **1995**, *242*, 304.
(27) Gregory, D. M.; Wolfe, G. M.; Jarvie, T. P.; Sheils, J. C.; Drobny, G. P. *Mol. Phys.* **1996**, *89*, 1835.
(28) Costa, P. R.; Sun, B.; Griffin, R. G. *J. Am. Chem. Soc.* **1997**, *119*, 10821.
(29) Verel, R.; Baldus, M.; Nijman, M.; van Os, J. W. M.; Meier, B. H. *Chem. Phys. Lett.* **1997**, *280*, 31.
(30) Hohwy, M.; Rienstra, C. M.; Jaroniec, C. P.; Griffin, R. G. *J. Chem. Phys.* **1999**, *110*, 7983.
(31) Jarrell, H. C.; Siminovitch, D. *Chem. Phys. Lett.* **1999**, *314*, 421.
(32) (a) Raleigh, D. P.; Creuzet, F.; Das Gupta, S. K.; Levitt, M. H.; Griffin, R. G. *J. Am. Chem. Soc.* **1989**, *111*, 4502. (b) Creuzet, F.; McDermott, A.; Gebhard, R.; van der Hoef, K.; Spijker-Assink, M. B.; Herzfeld, J.; Lugtenburg, J.; Levitt, M. H.; Griffin, R. G. *Science* **1991**, *251*, 783. (c) Lakshmi, K. V.; Auger, M.; Raap, J.; Lugtenburg, J.; Griffin, R. G.; Herzfeld, J. *J. Am. Chem. Soc.* **1993**, *115*, 8515. (d) Smith, S. O. *Curr. Opin. Struct. Biol.* **1993**, *3*, 755. (e) Smith, S. O.; Hamilton, J.; Salmon, A.; Bormann, B. J. *Biochemistry* **1994**, *33*, 6327. (f) Challoner, R.; Harris, R. K. *Chem. Phys. Lett.* **1994**, *228*, 589. (g) Karlsson, T.; Helmle, M.; Kurur, N. D.; Levitt, M. H. *Chem. Phys. Lett.* **1995**, *247*, 534. (h) Griffiths, J. M.; Ashburn, T. T.; Auger, M.; Costa, P. R.; Griffin, R. G.; Lansbury, P. T., Jr. *J. Am. Chem. Soc.* **1995**, *117*, 3539. (i) Peersen, O. B.; Groesbeek, M.; Aimoto, S.; Smith, S. O. *J. Am. Chem. Soc.* **1995**, *117*, 7228. (j) Auger, M. *J. Chim. Phys.* **1995**, *92*, 1751. (k) Verdegem, P. J. E.; Helmle, M.; Lugtenburg, J.; de Groot, H. J. M. *J. Am. Chem. Soc.* **1997**, *119*, 169. (l) Koons, J. M.; Pavlovskaya, G. E.; Jones, A. A.; Inglefield, P. T. *J. Magn. Reson.* **1997**, *124*, 499. (m) Nomura, K.; Takegoshi, K.; Terao, T.; Uchida, K.; Kainosho, M. *J. Am. Chem. Soc.* **1999**, *121*, 4064. (n) Feng, X.; Verdegem, P. J. E.; Lee, Y. K.; Helmle, M.; Shekar, S. C.; de Groot, H. J. M.; Lugtenburg, J.; Levitt, M. H. *Solid State Nucl. Magn. Reson.* **1999**, *14*, 81.
(33) Kundla, E.; Heinmaa, I.; Kooskora, H.; Lippmaa, E. *J. Magn. Reson.* **1997**, *129*, 53.
(34) Peersen, O. B.; Smith, S. O. *Concepts Magn. Reson.* **1993**, *5*, 303.
(35) Raleigh, D. P.; Kolbert, A. C.; Oas, T. G.; Levitt, M. H.; Griffin, R. G. *J. Chem. Soc., Faraday Trans. 1* **1988**, *84*, 3691.

(36) Costa, P. R.; Kocisko, D. A.; Sun, B. Q.; Lansbury, P. T., Jr.; Griffin, R. G. *J. Am. Chem. Soc.* **1997**, *119*, 10487.
(37) Levitt, M. H.; Raleigh, D. P.; Creuzet, F.; Griffin, R. G. *J. Chem. Phys.* **1990**, *92*, 6347.
(38) Lansbury, P. T., Jr.; Costa, P. R.; Griffiths, J. M.; Simon, E. J.; Auger, M.; Halverson, K. J.; Kocisko, D. A.; Hendsch, Z. S.; Ashburn, T. T.; Spencer, R. G. S.; Tidor, B.; Griffin, R. G. *Nat. Struct. Biol.* **1995**, *2*, 990.
(39) McDermott, A. E.; Creuzet, F.; Griffin, R. G.; Zawadzke, L. E.; Ye, Q.-Z.; Walsh, C. T. *Biochemistry* **1990**, *29*, 5767.
(40) Tomita, Y.; O'Connor, E. J.; McDermott, A. *J. Am. Chem. Soc.* **1994**, *116*, 8766.
(41) Thompson, L. K.; McDermott, A. E.; Raap, J.; van der Wielen, C. M.; Lugtenburg, J.; Herzfeld, J.; Griffin, R. G. *Biochemistry* **1992**, *31*, 7931.
(42) Smith, S. O.; Jonas, R.; Braiman, M.; Bormann, B. J. *Biochemistry* **1994**, *33*, 6334.
(43) Smith, S. O.; Bormann, B. J. *Proc. Natl. Acad. Sci. U.S.A.* **1995**, *92*, 488.
(44) Peersen, O. B.; Yoshimura, S.; Hojo, H.; Aimoto, S.; Smith, S. O. *J. Am. Chem. Soc.* **1992**, *114*, 4332.
(45) Helmle, M.; Lee, Y. K.; Verdegem, P. J. E.; Feng, X.; Karlsson, T.; Lugtenburg, J.; de Groot, H. J. M.; Levitt, M. H. *J. Magn. Reson.* **1999**, *140*, 379.
(46) Middleton, D. A.; Le Duff, C. S.; Peng, X.; Reid, D. G.; Saunders: D. *J. Am. Chem. Soc.* **2000**, *122*, 1161.
(47) Spencer, R. G. S.; Fishbein, K. W.; Levitt, M. H.; Griffin. R. G. *J. Chem. Phys.* **1994**, *100*, 5533.
(48) Nijman, M.; Ernst, M.; Kentgens, A. P. M.; Meier, B. H. *Mol. Phys.* **2000**, *98*, 161.
(49) Baldus, M.; Rovnyak, D.; Griffin, R. G. *J. Chem. Phys.* **2000**, *112*, 5902.
(50) Hodgkinson, P.; Emsley, L. *J. Magn. Reson.* **1999**, *139*, 46.
(51) Dusold, S.; Maisel, H.; Sebald, A. *J. Magn. Reson.* **1999**, *141*, 78.
(52) (a) Zilm, K. W.; Webb, G. G.; Cowley, A. H.; Pakulski, M.; Orendt, A. *J. Am. Chem. Soc.* **1988**, *110*, 2032. (b) Nakai, T.; McDowell, C. A. *J. Am. Chem. Soc.* **1994**, *116*, 6373.
(53) For example, see: (a) *Nuclear Magnetic Shieldings and Molecular Structure*; Tossell, J. A., Ed.; NATO Series C: Mathematical and Physical Sciences; Kluwer Academic Publishers: Dordrecht, Germany, 1993; Vol. 386. (b) *Modeling NMR Chemical Shifts: Gaining Insights into Structure and Environment*; Facelli, J. C., de Dios, A. C., Eds.; ACS Symposium Series 732; American Chemical Society: Washington, D.C., 1999. (c) Annual reviews: Jameson, C. J.; de Dios, A. C. In *Nuclear Magnetic Resonance: A Specialist Periodical Report*; Webb, G. A., Ed.; Royal Society of Chemistry: Cambridge, U.K.
(54) Grant, D. M.; Facelli, J. C.; Alderman, D. W.; Sherwood, M. H. In ref 53a, pp 367−384.
(55) van Willigen, H.; Griffin, R. G.; Haberkorn, R. A. *J. Chem. Phys.* **1977**, *67*, 5855.
(56) We refer here only to the symmetric part of the CS tensor. The antisymmetric portion is known to have a negligible contribution to the NMR spectrum. (a) Anet, F. A. L.; O'Leary, D. J. *Concepts Magn. Reson.* **1991**, *3*, 193 (b) Anet, F. A. L.; O'Leary, D. J. *Concepts Magn. Reson.* **1992**, *4*, 35 (c) Ding, S.; Ye, C. *Chem. Phys. Lett.* **1990**, *170*, 277 (d) Haeberlen, U. In *Advances in Magnetic Resonance*; Waugh, J. S., Ed.; Academic Press: New York, 1976; Supplement 1, Chapter III.
(57) Kaski, J.; Lantto, P.; Vaara, J.; Jokisaari, J. *J. Am. Chem. Soc.* **1998**, *120*, 3993.
(58) (a) Wasylishen, R. E.; Wright, K. C.; Eichele, K.; Cameron, T. S. *Inorg. Chem.* **1994**, *33*, 407. (b) Lumsden, M. D.; Wasylishen, R. E.; Britten, J. F. *J. Phys. Chem.* **1995**, *99*, 16602. (c) Bryce, D. L.; Wasylishen, R. E. *J. Am. Chem. Soc.* **2000**, *122*, 3197.
(59) (a) Ishii, Y.; Terao, T.; Hayashi, S. *J. Chem. Phys.* **1997**, *107*, 2760. (b) Henry, E. R.; Szabo, A. *J. Chem. Phys.* **1985**, *82*, 4753. (c) Millar, J. M.; Thayer, A. M.; Zax, D. B.; Pines, A. *J. Am. Chem. Soc.* **1986**, *108*, 5113. (d) Nakai, T.; Ashida, J.; Terao, T. *Mol. Phys.* **1989**, *67*, 839.
(60) Mason, J. *Solid State Nucl. Magn. Reson.* **1993**, *2*, 285.
(61) Karlsson, T.; Levitt, M. H. *J. Chem. Phys.* **1998**, *109*, 5493.
(62) See, for example: Eichele, K.; Ossenkamp, G. C.; Wasylishen, R. E.; Cameron, T. S. *Inorg. Chem.* **1999**, *38*, 639.
(63) Bacon, G. E.; Walker, C. R.; Speakman, J. C. *J. Chem. Soc., Perkin Trans. II* **1977**, 979.
(64) Bennett, A. E.; Rienstra, C. M.; Auger, M.; Lakshmi, K. V.; Griffin, R. G. *J. Chem. Phys.* **1995**, *103*, 6951.
(65) Bodenhausen, G.; Freeman, R.; Morris, G. A. *J. Magn. Reson.* **1976**, *23*, 171.
(66) Geen, H.; Levitt, M. H.; Bodenhausen, G. *Chem. Phys. Lett.* **1992**, *200*, 350.
(67) Eichele, K.; Wasylishen, R. E. *WSOLIDS1 NMR Simulation Package*, version 1.17.21; Dalhousie University: Halifax, Canada, 1998.
(68) Eichele, K.; Wasylishen, R. E. *Spin−Echo Simulation Package*, Version 1.1.6; Dalhousie University: Halifax, Canada, 1998.
(69) Alderman, D. W.; Solum, M. S.; Grant, D. M. *J. Chem. Phys.* **1986**, *84*, 3717.
(70) Sun, B.-Q.; Griffin, R. G. *NMRLAB*, unpublished simulation program.
(71) Lee, Y. K.; Levitt, M. H. *cc2z*, a program for simulating Zeeman magnetization exchange curves; Stockholm University: Stockholm, Sweden, 1990.
(72) Frisch, M. J.; Trucks, G. W.; Schlegel, H. B.; Scuseria, G. E.; Robb, M. A.; Cheeseman, J. R.; Zakrzewski, V. G.; Montgomery, J. A., Jr.; Stratmann, R. E.; Burant, J. C.; Dapprich, S.; Millam, J. M.; Daniels, A. D.; Kudin, K. N.; Strain, M. C.; Farkas, O.; Tomasi, J.; Barone, V.; Cossi, M.; Cammi, R.; Mennucci, B.; Pomelli, C.; Adamo, C.; Clifford, S.; Ochterski, J.; Petersson, G. A.; Ayala, P. Y.; Cui, Q.; Morokuma, K.; Malick, D. K.; Rabuck, A. D.; Raghavachari, K.; Foresman, J. B.; Cioslowski, J.; Ortiz, J. V.; Stefanov, B. B.; Liu, G.; Liashenko, A.; Piskorz, P.; Komaromi, I.; Gomperts, R.; Martin, R. L.; Fox, D. J.; Keith, T.; Al-Laham, M. A.; Peng, C. Y.; Nanayakkara, A.; Gonzalez, C.; Challacombe, M.; Gill, P. M. W.; Johnson, B. G.; Chen, W.; Wong, M. W.; Andres, J. L.; Head-Gordon, M.; Replogle, E. S.; Pople, J. A. *Gaussian 98*, revision A.4; Gaussian, Inc.: Pittsburgh, PA, 1998.
(73) Hodgson, D. J.; Asplund, R. O. *Acta Crystallogr.* **1991**, *C47*, 1986.
(74) Jeffrey, G. A.; Ruble, J. R.; McMullan, R. K.; Pople, J. A. *Proc. R. Soc. London A* **1987**, *414*, 47.
(75) (a) Ditchfield, R. *Mol. Phys.* **1974**, *27*, 789. (b) Wolinski, K.; Hinton, J. F.; Pulay, P. *J. Am. Chem. Soc.* **1990**, *112*, 8251.
(76) Basis sets were obtained from the Extensible Computational Chemistry Environment Basis Set Database (http://www.emsl.pnl.gov:2080/forms/basisform.html), as developed and distributed by the Molecular Science Computing Facility, Environmental and Molecular Sciences Laboratory, which is part of the Pacific Northwest Laboratory, P.O. Box 999, Richland, WA 99352, and is funded by the U.S. Department of Energy. The Pacific Northwest Laboratory is a multi-program laboratory operated by Battelle Memorial Institute for the U.S. Department of Energy under contract DE-AC06−76RLO 1830. Contact David Feller or Karen Schuchardt for further information.
(77) (a) Jameson, A. K.; Jameson, C. J. *Chem. Phys. Lett.* **1987**, *134*, 461. (b) Jameson, C. J. In *Encyclopedia of Nuclear Magnetic Resonance*; Grant, D. M., Harris, R. K., Eds.; Wiley, Inc.: Chichester, U.K., 1996; pp 1273−1281. (c) An alternative ^{13}C shielding scale has been proposed: Raynes, W. T.; McVay, R.; Wright, S. J. *J. Chem. Soc., Faraday Trans. 2* **1989**, *85*, 759.
(78) Herzfeld, J.; Berger, A. E. *J. Chem. Phys.* **1980**, *73*, 6021.
(79) Facelli, J. C.; Gu, Z.; McDermott, A. *Mol. Phys.* **1995**, *86*, 865.
(80) Gu, Z.; Zambrano, R.; McDermott, A. *J. Am. Chem. Soc.* **1994**, *116*, 6368.
(81) Schröter, B.; Rosenberger, H.; Hadži, D. *J. Mol. Struct.* **1983**, *96*, 301.
(82) Wilson, C. C.; Shankland, N.; Florence, A. J. *Chem. Phys. Lett.* **1996**, *253*, 103.
(83) Jeffrey, G. A. *An Introduction to Hydrogen Bonding*; Oxford University Press: Oxford, U.K., 1997.
(84) Schmidt-Rohr, K.; Spiess, H. W. *Multidimensional Solid-State NMR and Polymers*; Academic Press: London, 1994; pp 38−39.
(85) For examples of the importance of intermolecular effects in the calculation of NMR parameters, see: (a) Vaara, J.; Kaski, J.; Jokisaari, J.; Diehl, P. *J. Phys. Chem. A* **1997**, *101*, 5069. (b) Orendt, A. M.; Facelli, J. C.; Grant, D. M. *Chem. Phys. Lett.* **1999**, *302*, 499.
(86) Jameson, C. J. In *Multinuclear NMR*; Mason, J., Ed.; Plenum Press: New York, 1987; Chapter 3.
(87) Jarret, R. M.; Cusumano, L.; Dinztner, M.; Fortin, M.; Pothier, K.; Connolly, J.; Biondi, M.; Morrison, T. *Microchem. J.* **1993**, *47*, 187.
(88) Clegg, W.; Little, I. R.; Straughan, B. P. *Acta Crystallogr.* **1986**, *C42*, 1701.
(89) Meier, B. H.; Earl, W. L. *J. Am. Chem. Soc.* **1987**, *109*, 7937. Meier and Earl make explicit reference to the dihydrate form, whereas in other papers (e.g., refs 15 and 37), it is not clear whether the anhydrous form or the dihydrate form is being studied.
(90) Mehring, M. *Principles of High-Resolution NMR in Solids*, 2nd ed.; Springer-Verlag: Berlin, 1983; Section 7.5.